Modeling the geophysical history of very large impact basins: The gravity anomalies of the Orientale basin

David M. Blair[1]*, Brandon C. Johnson[2], Andrew M. Freed[1], and H. Jay Melosh[1]

* Point of Contact: **dblair@purdue.edu**. [1] Department of Earth and Atmospheric Sciences, Purdue University, West Lafayette, IN; [2] Department of Earth, Atmospheric and Planetary Sciences, Massachusetts Institute of Technology, Cambridge, MA.

Abstract

ePoster

Introduction

The **gravity anomalies of lunar impact basins** form via a combination of syn- and post-impact processes [1].

Modeling the formation of these anomalies therefore allows us to learn more about both the **parameters of the impact** and the **geophysical environment** in which the basin evolved.

In this study, we look at the lunar **Orientale Basin**, which, at a diameter of ~960 km, is large enough that the **curvature of the Moon** may have affected its formation and evolution.

Orientale Basin, located on the eastern limb of the Moon, is the youngest and best-preserved multi-ringed impact basin on the lunar surface This Lunar Orbiter IV image [2] shows the three major ring faults around Orientale.

Observational Constraints

We use **free-air and Bouguer gravity anomaly maps** from NASA's dual *Gravity Reconnaissance And Interior Laboratory* (**GRAIL**) spacecraft [3], and **topography** from the Lunar Orbital Laser Altimeter instrument aboard NASA's *Lunar Reconnaissance Orbiter* (**LRO/LOLA**) [4]. Our **crustal thickness** data comes from an inversion of GRAIL data [5].

All data is **azimuthally averaged** along small circles centered on Orientale (at 266.0ºE, 19.4ºS). We report both the mean and 2σ error in the plots below; the error arises from **real asymmetry** in the basin.

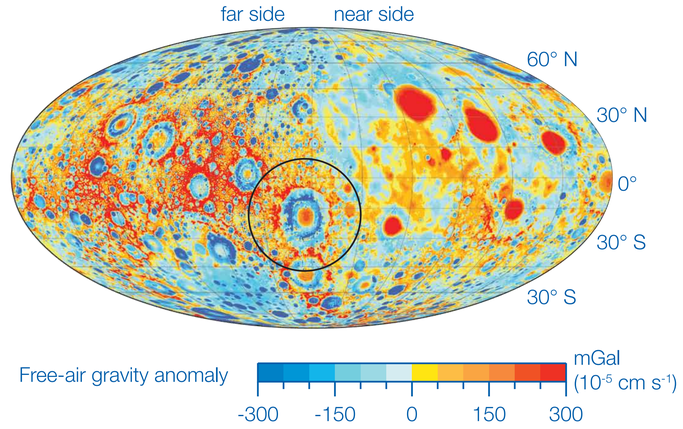

Global free-air gravity anomaly data from GRAIL [2] shows that Orientale (circled in black) displays a "bull's-eye" gravity pattern also seen in many other basins on both the near and far sides of the Moon.

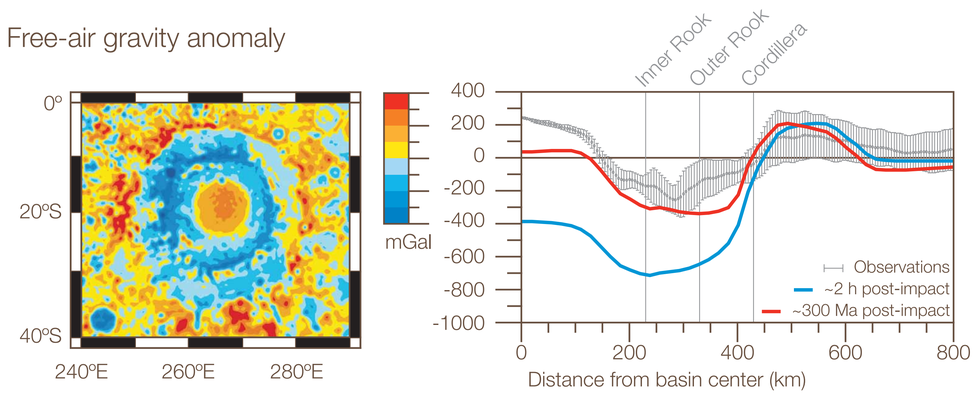

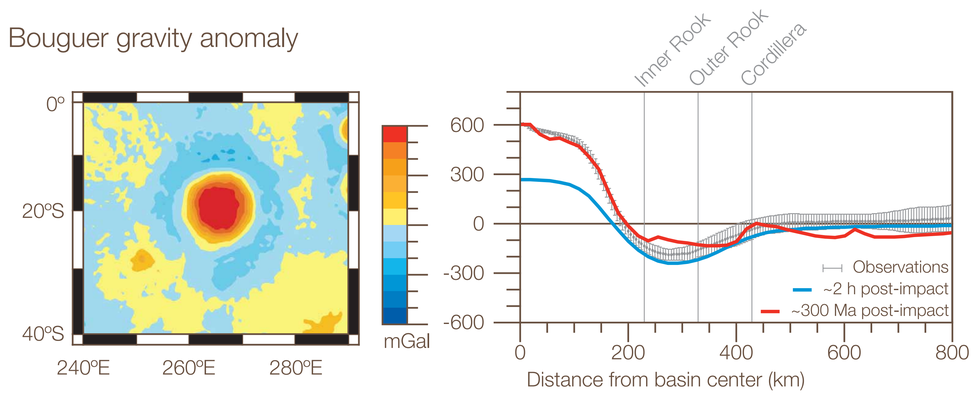

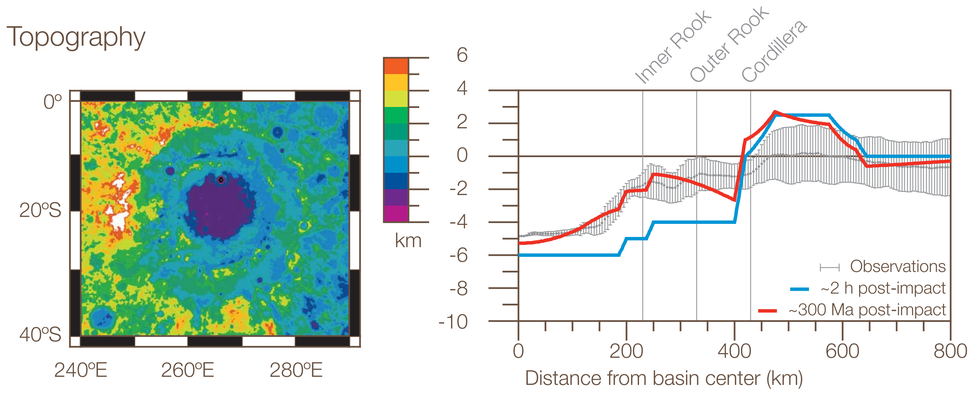

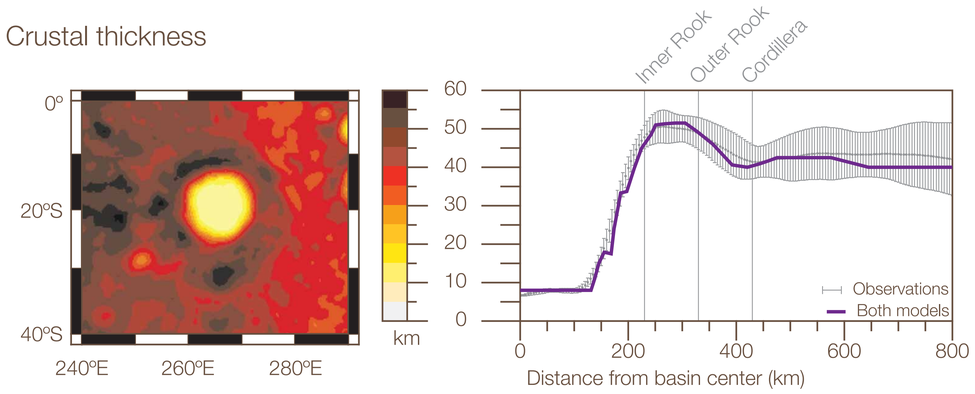

Results from one of our preliminary models of the geophysical evolution of Orientale basin, showing comparisons to a variety of observational datasets. Blue lines are from shortly after impact (at the end of the iSALE simulation), while red lines represent the state of the basin ~300 Ma later (at the end of the finite element model).

Modeling & Results

The **entire history** of the Orientale basin from the moment of impact through geophysical evolution can be explored by using a **multi-stage modeling approach** [1, 6, 7], shown below.

First, we simulate the basin-forming impact using the **iSALE hydrocode** [e.g. 7, 8], varying the pre-impact crustal thickness, subsurface thermal gradient, and the kinetic energy of the impactor as required.

We then model the cooling and isostatic relaxation of the basin using the **Abaqus finite-element modeling** program, using the end state of the hydrocode model as the initial conditions for our model.

The models shown at left are **a work in progress**; we do not yet have a model that matches all of the constraints.

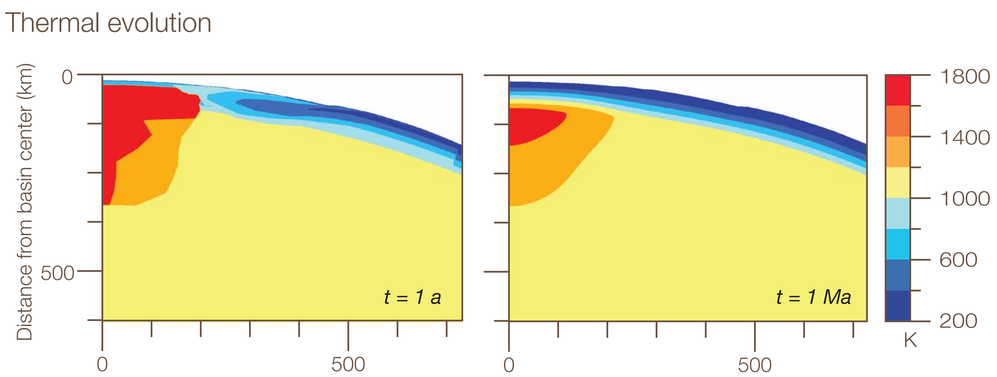

Temperatures during a finite element simulation, showing the initial state and a point before the subsurface has fully cooled (typically ~10 Ma after impact). Because our models use a temperature and pressure-dependent rheology, the thermal structure has a substantial effect on our final result.

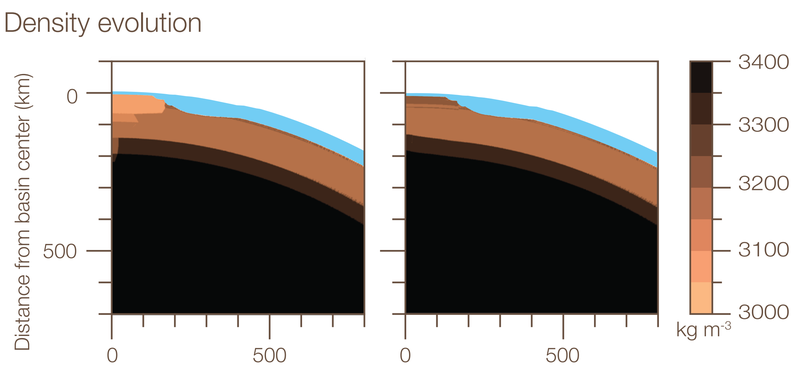

Thermal contraction leads to a large change in density in the melt pool under the Orientale basin over the course of a ~300 Ma finite element simulation. Colors represent densities in the melt pool and mantle; the crust is shown in blue for reference.

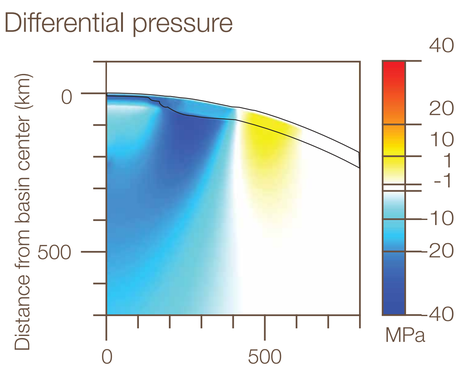

The difference between pressure under Orientale and normal lithostatic pressure plays a large role in driving relaxation and viscous flow.

References & Acknowledgements

[1] Melosh, H. J., et al. (2013) Science 340; [2] NASA/USGS/LPI, Lunar Orbiter IV image 4187_med; [3] Zuber, M. T., et al. (2013) Science 339; [4] Neumann, G.A. (2010), NASA PDS; [5] Wieczorek, M. A. et al. (2013) Science 339; [6] Blair et al. (2013) LPSC 44; [7] Freed. A. M., et al. (2014), in prep.; [7] Amsden, A. A., et al. (1980), LANL Rep. LA-8095, 101; [8] Wünnemann, K., et al. (2006) Icarus 180; [9] Turtle, E. P., and Melosh, H. J. (1997), Icarus 126. This work is supported by NASA Headquarters under the NASA Earth and Space Science Fellowship Program, Grant NNX13AO63H, and also by the GRAIL mission.